Draft version August 14, 2013
Preprint typeset using LaTeX style emulateapj v. 11/10/09

ON MEASURING INNER HALO PROFILES WITH WEAK LENSING SHEAR AND MAGNIFICATION

Matthew R. George
Department of Astronomy, University of California, Berkeley and
Lawrence Berkeley National Laboratory, 1 Cyclotron Road, Berkeley, CA 94720, USA

Draft version August 14, 2013

ABSTRACT

Subject headings:

1. INTRODUCTION

We want to measure the shape of the dark matter profile on small scales. This will tell us how baryons have affected the dark matter distribution, the assembly history of the baryons and dark matter as well as feedback processes, and whether dark matter interacts to form "cored" profiles as opposed to the "cuspy" profiles seen in cold dark matter simulations. Measurements of the mass distribution on scales comparable to the effective radius of a galaxy can also constrain the mass-to-light ratio of the stellar population which is uncertain by a factor of ~ 2 depending on the initial mass function which is generally assumed.

Various observational probes have been used to constrain the mass profile of galaxies and dark matter halos, typically with dynamical measurements within a few kpc of the galaxy center, stong lensing arcs a bit farther out, and weak lensing on larger scales to measure the total mass of the halo (e.g., Sand et al. 2004; Koopmans et al. 2006; Gavazzi et al. 2007; Jiang & Kochanek 2007; Auger et al. 2010; Schulz et al. 2010; Newman et al. 2013). While central velocity dispersions or rotation curves can be measured for large samples of galaxies, detailed kinematic measures on scales $\gtrsim 10$ kpc are difficult and strong lenses exist in only a sparse sample of the galaxy population. Weak lensing, on the other hand, can probe the average profile for large samples of galaxies, allowing studies of population differences and redshift evolution, independent of their dynamical state. For instance, the assembly histories of disk and elliptical galaxies may differ and hydrodynamical simulations predict significant differences in the inner profiles of their dark matter halos. The aim of this letter is to investigate how well weak lensing shear and magnification can constrain the inner mass profile of dark matter halos and galaxies.

Several authors have studied the complementarity of shear and magnification, primarily for measuring halo masses (Bartelmann et al. 1996; Bridle et al. 1998; Schneider et al. 2000; van Waerbeke et al. 2010; Rozo & Schmidt 2010; Umetsu et al. 2011) or probing the matter distribution on cosmological scales (van Waerbeke 2010; Casaponsa et al. 2013; Duncan et al. 2013; Krause et al. 2013). Combining shear and magnification increases the statistical precision of a lensing experiment and also enables tests of systematic effects which differ between probes.

Magnification can be measured using sizes (Bartelmann & Narayan 1995), fluxes (Broadhurst et al. 1995), or by combining the two (Huff & Graves 2011; Schmidt et al. 2012). Magnification has recently been measured with signal-to-noise approaching that from shear for ensembles of galaxies (Scranton et al. 2005; Hildebrandt et al. 2009; Ménard et al. 2010; Huff & Graves 2011; Ford et al. 2012; Schmidt et al. 2012).

Electronic address: mgeorge@astro.berkeley.edu

2. LENS MODELING

The distortion of galaxy images due to weak lensing can be described by a matrix written in terms of the convergence κ and shear components γ_1, γ_2 (e.g. Bartelmann & Schneider 2001):

$$A = \begin{pmatrix} 1-\kappa-\gamma_1 & -\gamma_2 \\ -\gamma_2 & 1-\kappa+\gamma_1 \end{pmatrix}. \quad (1)$$

From galaxy images, one can measure the magnification $\mu = (\det \mathrm{A})^{-1} = [(1-\kappa)^2 - |\gamma|^2]^{-1} \approx 1+2\kappa$ and reduced shear $g = \gamma/(1-\kappa) \approx \gamma$, where we have defined the complex shear $\gamma = \gamma_1 + i\gamma_2$ and approximations are given to first order in the weak limit $|\gamma|, \kappa \ll 1$.

The convergence and tangential component of shear can be related to the projected surface mass density Σ of the lens via

$$\kappa = \frac{\Sigma}{\Sigma_c}; \;\; \gamma_t = \frac{\Delta\Sigma}{\Sigma_c} \quad (2)$$

where the critical surface density Σ_c is a function of the angular diameter distances between the observer (O), lens (L), and source (S),

$$\Sigma_c = \frac{c^2}{4\pi G}\frac{D_{OS}}{D_{OL}D_{LS}}. \quad (3)$$

A typical experiment averages measurements of g_t or κ in bins of radius R around the lens position to constrain its radial surface density profile (or stacks many such measurements for an ensemble of lenses). Magnification directly probes the surface density at a given position $\Sigma(R)$, whereas shear is sensitive to the excess surface density interior to the projected radius $\Delta\Sigma(R) = \overline{\Sigma}(<R) - \overline{\Sigma}(R)$. This difference in scale-dependence is what we hope to exploit by combining shear and magnification measurements to constrain inner halo profiles.

We shall assume that Σ and $\Delta\Sigma$ can be estimated from magnification and shear observables in an unbiased manner down to our minimum radius (typically 40 kpc which is $\sim 20''$ at $z_L = 0.1$). For discussion of modeling lensing observables into the nonlinear regime, see Ménard et al. (2003); Takada & Hamana (2003); Mandelbaum et al.

(2006). We will also assume these quantities are constrained independently; see Rozo & Schmidt (2010) for a treatment of their covariance.

NFW, gNFW, AC models.

Assumptions: neglect covariance, systematics. Reduced shear? Non-weak lensing? Relative S/N of shear vs. magnification. No contraction beyond virial radius, extrapolation with NFW.

Plots of rho, sigma, delta sigma.

3. FORECASTS

Results. Choice of fiducial system(s) - galaxy vs cluster, concentration, mention miscentering.

Priors

Plots of constraints.

4. CONCLUSIONS

REFERENCES

Auger, M. W., Treu, T., Bolton, A. S., Gavazzi, R., Koopmans, L. V. E., Marshall, P. J., Moustakas, L. A., & Burles, S. 2010, ApJ, 724, 511

Bartelmann, M., & Narayan, R. 1995, ApJ, 451, 60

Bartelmann, M., Narayan, R., Seitz, S., & Schneider, P. 1996, ApJ, 464, L115

Bartelmann, M., & Schneider, P. 2001, Phys. Rep., 340, 291

Bridle, S. L., Hobson, M. P., Lasenby, A. N., & Saunders, R. 1998, MNRAS, 299, 895

Broadhurst, T. J., Taylor, A. N., & Peacock, J. A. 1995, ApJ, 438, 49

Casaponsa, B., Heavens, A. F., Kitching, T. D., Miller, L., Barreiro, R. B., & Martínez-González, E. 2013, MNRAS, 430, 2844

Duncan, C., Joachimi, B., Heavens, A., Heymans, C., & Hildebrandt, H. 2013, ArXiv e-prints

Ford, J., et al. 2012, ApJ, 754, 143

Gavazzi, R., Treu, T., Rhodes, J. D., Koopmans, L. V. E., Bolton, A. S., Burles, S., Massey, R. J., & Moustakas, L. A. 2007, ApJ, 667, 176

Hildebrandt, H., van Waerbeke, L., & Erben, T. 2009, A&A, 507, 683

Huff, E. M., & Graves, G. J. 2011, ArXiv e-prints

Jiang, G., & Kochanek, C. S. 2007, ApJ, 671, 1568

Koopmans, L. V. E., Treu, T., Bolton, A. S., Burles, S., & Moustakas, L. A. 2006, ApJ, 649, 599

Krause, E., Chang, T.-C., Doré, O., & Umetsu, K. 2013, ApJ, 762, L20

Mandelbaum, R., Seljak, U., Cool, R. J., Blanton, M., Hirata, C. M., & Brinkmann, J. 2006, MNRAS, 372, 758

Ménard, B., Hamana, T., Bartelmann, M., & Yoshida, N. 2003, A&A, 403, 817

Ménard, B., Scranton, R., Fukugita, M., & Richards, G. 2010, MNRAS, 405, 1025

Newman, A. B., Treu, T., Ellis, R. S., Sand, D. J., Nipoti, C., Richard, J., & Jullo, E. 2013, ApJ, 765, 24

Rozo, E., & Schmidt, F. 2010, ArXiv e-prints

Sand, D. J., Treu, T., Smith, G. P., & Ellis, R. S. 2004, ApJ, 604, 88

Schmidt, F., Leauthaud, A., Massey, R., Rhodes, J., George, M. R., Koekemoer, A. M., Finoguenov, A., & Tanaka, M. 2012, ApJ, 744, L22

Schneider, P., King, L., & Erben, T. 2000, A&A, 353, 41

Schulz, A. E., Mandelbaum, R., & Padmanabhan, N. 2010, MNRAS, 408, 1463

Scranton, R., et al. 2005, ApJ, 633, 589

Takada, M., & Hamana, T. 2003, MNRAS, 346, 949

Umetsu, K., Broadhurst, T., Zitrin, A., Medezinski, E., & Hsu, L.-Y. 2011, ApJ, 729, 127

van Waerbeke, L. 2010, MNRAS, 401, 2093

van Waerbeke, L., Hildebrandt, H., Ford, J., & Milkeraitis, M. 2010, ApJ, 723, L13

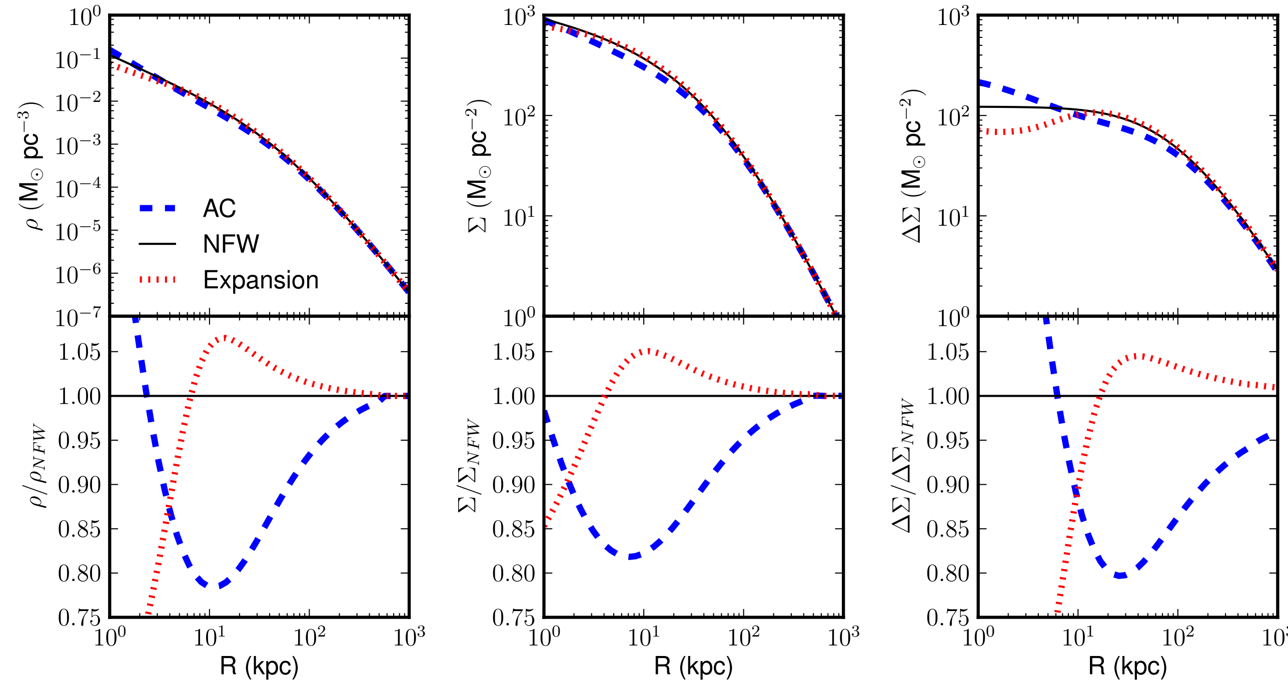

FIG. 1.— Density profiles for different halo models.